References

1. Orešković D, Klarica M. The formation of cerebrospinal fluid: Nearly a hundred years of interpretations and misinterpretations. Brain Res. Rev., 2010;64: 241-262.
2. Igarashi H, Tsujita M, Kwee IL, Nakada T. Water Influx into Cerebrospinal Fluid (CSF) is Primarily Controlled by Aquaporin-4, not by Aquaporin-1: O-17 JJVCPE MRI Study in Knockout Mice. Neuroreport 2014;25:39-43.
3. Haj-Yasein NN, Jensen V, Østby I, Omholt SW, Voipio J, Kaila K, et al. Aquaporin-4 regulates extracellular space volume dynamics during high-frequency synaptic stimulation: A gene deletion study in mouse hippocampus. Glia. 2012;60:867-874.
4. Johnston M, Papaiconomou C. Cerebrospinal fluid transport: a lymphatic perspective. News Physiol Sci 2002;17 :227-230
5. Abott NJ. Evidence for bulk flow of brain interstitial fluid: significance for physiology and pathology. Neurochem Int 2004;45:545-552
6. Weller RO, Djuanda E, Yow HY, CarareRO. Lymphatic drainage of the brain and the pathophysiology of neurological disease. Acta Neuropathol 2009;117:1-14
7. Iliff JJ, Wang M, Liao Y, Plogg BA, Peng W, Gundersen GA, et al. A paravascular pathway facilitates CSF flow through the brain parenchyma and the clearance of interstitial solutes, including amyloid β. Sci Transl Med 2012;4;147ra111
8. Weller RO. Pathology of cerebrospinal fluid and interstitial fluid of the CNS: significance for Alzheimer disease, prion disorders and multiple sclerosis. J Neuropathol Exp Neurol 1998;57:885–894
9. Xinyi L, Buxbaum JN, Transthyretin and the brain re-visited: Is neuronal synthesis of transthyretin protective in Alzheimer's disease? Neurodegeneration 2011; 6 :79.
10. Kitaura H, Tsujita M, Huber VJ, Kakita A, Shibuki K, Sakimura K, et al. Activity-dependent glial swelling is impaired in aquaporin-4 knockout mice. Neurosci Res 2009;64: 208-212.
11. Nakada T., Grant-in-Aid for Scientific Research (S). Integrated Science and Innovative Science. Magnetic resonance molecular microimaging. (2007) http://www.jsps.go.jp/j-grantsinaid/12_kiban/ichiran_21/e-data/e07_nakada.pdf
12. Suzuki K, Igarashi H, Huber VJ, Kitaura H, Kwee IL, Nakada T. Ligand based molecular MRI: O-17 JJVCPE amyloid imaging in transgenic mice. J. Neuroimag. 23 February 2014 DOI: 10.1111/jon.12091.
13. Igarashi H, Suzuki Y, Kwee IL, Nakada T. Water Influx into cerebrospinal fluid is

significantly reduced in senile plaque bearing transgenic mice, supporting β-Amyloid clearance hypothesis of Alzheimer's disease. Neurol Res (In Press)

14. Nakada T. Review: Virchow-Robin space and aquaporin-4: New insights on an old friend. Croatian Med J (In Press)
15. Virchow R. Ueber die Erweiterung kleinerer Gefaesse. Arch Pathol Anat Physiol Klin Med 1851;3:427-462
16. Robin C. Recherches sur quelques particularites de la structure des capillaires de l'encephale. J Physiol Homme Animaux 1859;2:537-548
17. Esiri MM, Gay D. Immunological and neuropathological significance of the Virchow-Robin space. J Neurol Sci 1990;100:3-8
18. Lulu X, Kang H, Xu Q, Chen MJ, Liao Y, Thiyagarajan M et al. Sleep drives metabolite clearance from the adult brain. Science 2013;342:373-377
19. Igarashi H, Tsujita M, Huber VJ, Kwee IL, Nakada T. Inhibition of Aquaporin-4 significantly increases regional cerebral blood flow. NeuroReport 2013;24:324-328
20. Huber VJ, Tsujita M, Nakada T. Aquaporins in drug discovery and pharmacotherapy. Mol Aspects Med 2012;33: 691-703
21. Dolman D, Drndarski S, Abbott NJ, Rattray M. Induction of aquaporin 1 but not aquaporin 4 messenger RNA in rat primary brain microvessel endothelial cells in culture. J Neurochem 2005; 93:825-833
22. Parihar MS, Brewer GJ. Amyloid-β as a modulator of synaptic plasticity. J Alzheimer's Dis. 2010;22:741-763

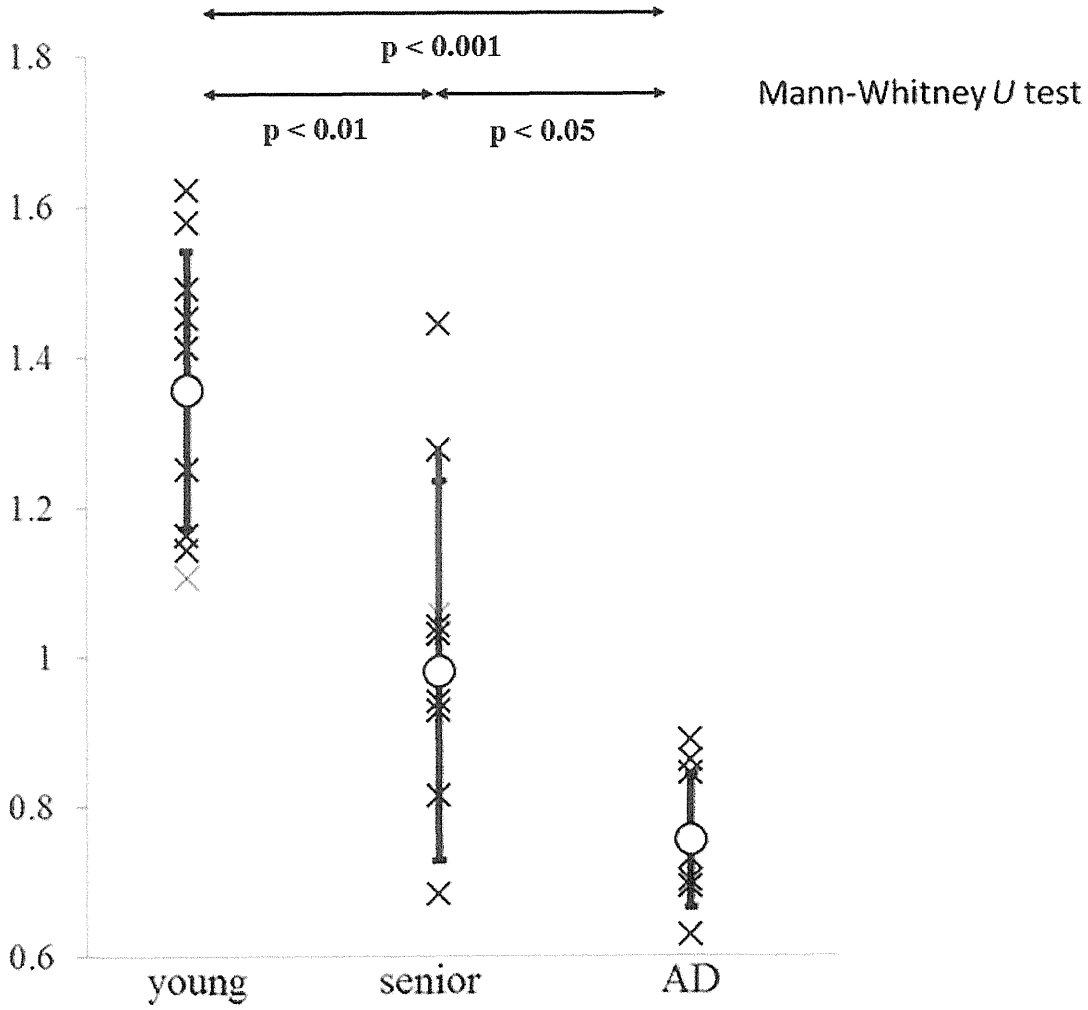
p < 0.001
p < 0.01
p < 0.05
Mann-Whitney U test
1.8
1.6
1.4
1.2
1
0.8
0.6
young
senior
AD

OPEN

Journal of Human Genetics (2015), 1–3

www.nature.com/jhg

SHORT COMMUNICATION

Systematic review and meta-analysis of Japanese familial Alzheimer's disease and FTDP-17

Kensaku Kasuga[1,2,6], Masataka Kikuchi[1,3,6], Takayoshi Tokutake[4], Akihiro Nakaya[1,5], Toshiyuki Tezuka[4], Tamao Tsukie[1,3], Norikazu Hara[1], Akinori Miyashita[1], Ryozo Kuwano[1] and Takeshi Ikeuchi[1]

Mutations in *APP*, *PSEN1* and *PSEN2* as the genetic causes of familial Alzheimer's disease (FAD) have been found in various ethnic populations. A substantial number of FAD pedigrees with mutations have been reported in the Japanese population; however, it remains unclear whether the genetic and clinical features of FAD in the Japanese population differ from those in other populations. To address this issue, we conducted a systematic review and meta-analysis of Japanese FAD and frontotemporal dementia with parkinsonism linked to chromosome 17 (FTDP-17) by literature search. Using this analysis, we identified 39 different *PSEN1* mutations in 140 patients, 5 *APP* mutations in 35 patients and 16 *MAPT* mutations in 84 patients. There was no *PSEN2* mutation among Japanese patients. The age at onset in Japanese FAD patients with *PSEN1* mutations was significantly younger than that in patients with *APP* mutations. Kaplan–Meier analysis revealed that patients with *MAPT* mutations showed a shorter survival than patients with *PSEN1* or *APP* mutations. Patients with mutations in different genes exhibit characteristic clinical presentations, suggesting that mutations in causative genes may modify the clinical presentations. By collecting and cataloging genetic and clinical information on Japanese FAD and FTDP-17, we developed an original database designated as Japanese Familial Alzheimer's Disease Database, which is accessible at http://alzdb.bri.niigata-u.ac.jp/.
Journal of Human Genetics advance online publication, 19 February 2015; doi:10.1038/jhg.2015.15

Mutations in *APP*, *PSEN1* and *PSEN2* as the genetic causes of familial Alzheimer's disease (FAD) have been found in various ethnic populations.[1,2] In addition, patients with mutations in *MAPT* associated with frontotemporal dementia with parkinsonism linked to chromosome 17 (FTDP-17) have been shown to exhibit Alzheimer's disease (AD)-like phenotypes.[3,4] Although a substantial number of FAD pedigrees have been reported in Japan, it is not yet clear whether the genetic and clinical features of FAD in the Japanese population differ from those in other ethnic populations. To characterize the genetic and clinical features of Japanese FAD and FTDP-17, we here performed a systematic review and meta-analysis, and developed an original database of Japanese FAD and FTDP-17.

To comprehensively review the previously reported Japanese FAD and FTDP-17 cases, we performed a systematic search for publications in PubMed and Ichushi, a bibliographic database of medical literature in Japanese. The terms 'familial Alzheimer', 'familial AD', 'FTDP-17', 'presenilin', '*PSEN1*', '*PSEN2*', '*APP*' and '*MAPT*' were used to search in PubMed, and the equivalent terms in Japanese were used to search in Ichushi. From the literature searches we found 60 English and 29 Japanese articles and/or abstracts that reported on Japanese FAD and FTDP-17 pedigrees bearing the causative mutations (Supplementary Table 1). Using the information obtained by the systematic literature review, we developed an original database for Japanese FAD and FTDP-17 designated as Japanese Familial Alzheimer's Disease database (JFADdb). In the database, each of the mutations in *APP*, *PSEN1/2*, *MAPT* and *GRN* was described in accordance with the reference sequences.[5] Information on age at onset, clinical manifestations, age at death and *APOE* genotype were included in the database (Supplementary Figure 1).

We identified 39 different *PSEN1* mutations in 140 patients, 5 *APP* mutations in 35 patients and 16 *MAPT* mutations in 84 patients (Table 1). Among them, 10 *PSEN1* mutations, 5 *APP* mutations and 11 *MAPT* mutations were not included in the well-known Alzheimer Disease and Frontotemporal Dementia Mutation database (http://www.molgen.ua.ac.be/ADMutations/).[6] No *PSEN2* mutation has been found in Japanese FAD. The frequency of mutated genes in FAD patients in the Japanese population was not significantly different from those in other populations (χ^2, $P=0.99$).[6] Most FAD pedigrees show autosomal dominant inheritance; however, an *APP* ΔE693 mutation was responsible for a recessively inherited FAD.[7] Sporadic occurrences of mutations were observed: five patients with *PSEN1* mutations, one patient with *APP* mutation and two patients with *MAPT* mutations.

[1]Department of Molecular Genetics, Brain Research Institute, Niigata University, Niigata, Japan; [2]Center for Transdisciplinary Research, Niigata University, Niigata, Japan; [3]Research Association for Biotechnology, Tokyo, Japan; [4]Department of Neurology, Brain Research Institute, Niigata University, Niigata, Japan and [5]Department of Genome Informatics, Graduate School of Medicine, Osaka University, Osaka, Japan
[6]These authors contributed equally to this work.
Correspondence: Dr T Ikeuchi, Department of Molecular Genetics, Brain Research Institute, Niigata University, 1-757 Asahimachi, Niigata 951-8585, Japan.
E-mail: ikeuchi@bri.niigata-u.ac.jp
Received 7 November 2014; revised 7 January 2015; accepted 13 January 2015

Table 1 Summary of genetic features of Japanese FAD and FTDP-17

Disease	Genes	Number of mutations	Number of pedigrees	Number of patients
FAD	*PSEN1*	39	40	140
	PSEN2	0	0	0
	APP	5[a]	13	35
FTDP-17	*MAPT*	16	29	84
	GRN	2	2	2

Abbreviations: FAD, familial Alzheimer's disease; FTDP-17, frontotemporal dementia with parkinsonism linked to chromosome 17.
[a]*APP* duplication was included.

In our analysis, the majority of mutations (73%) was observed in a single small pedigree. Considering that novel mutations in FAD tend to be reported rapidly, note that there may be publication bias in the frequency of mutations in the database. Although rare, there were two *GRN* mutations in patients with primary progressive aphasia and frontotemporal lobar degeneration (FTLD).[8] Because the number of *GRN* mutations was too small, the patients with *GRN* mutations were excluded from further meta-analysis.

The ages at onset were 44 ± 8 years (mean $\pm$ s.d.) in patients with *PSEN1* mutations ($n = 87$), 54 ± 9 years in *APP* mutations ($n = 23$) and 45 ± 10 years in *MAPT* mutations ($n = 51$). These ages at onset of FAD in our analysis are consistent with those reported in other ethnic populations.[6,9] The age at onset in patients with *APP* mutations was significantly older than those in patients with *PSEN1* or *MAPT* mutations (Figure 1a). The clinical phenotypes of patients with *MAPT* mutations were classified into three subgroups: FTLD,[10] AD-like[3,4] and progressive supranuclear palsy (PSP) phenotypes.[8] The age at onset in patients with the FTLD or PSP phenotype was significantly younger than that with the AD-like phenotype (Supplementary Figure 2). *APOE* genotypes did not significantly modify the age at onset in patients with causative mutations (Supplementary Figure 3). There was no significant difference in age at death among the patients with mutations in the three genes (Figure 1b). The disease duration from age at onset to death in patients with *MAPT* mutations was significantly shorter than that with *PSEN1* mutations (Figure 1c). The survival of patients after the onset was analyzed by Kaplan–Meier estimation, which revealed that patients with *MAPT* mutations showed a shorter survival than patients with *PSEN1* or *APP* mutations (Supplementary Figure 4).

The clinical diagnosis of AD before the genetic testing was performed in 96% of patients with *PSEN1* mutations and 97% of patients with *APP* mutations (Supplementary Table 2). Notably, only 57% of patients with *MAPT* mutations were clinically diagnosed as having FTLD; 19% and 12% of patients with *MAPT* mutations were clinically diagnosed as having AD and PSP, respectively (Supplementary Table 2). This finding suggests that mutational screening of clinically diagnosed FAD patients should not only include *APP* and *PSEN1/2* mutations but also include *MAPT* mutations.

We next analyzed the frequency of each of the clinical manifestations including psychiatric symptoms, mood disorders, spastic paraparesis, parkinsonism and epilepsy/seizure (Figure 2). As expected, the frequencies of psychiatric symptoms and parkinsonism were significantly higher in patients with *MAPT* mutations. Spastic paraparesis, which is a characteristic symptom of 'variant AD with cotton-wool plaque pathology'[11,12] was observed in 15% of patients with *PSEN1* mutations, whereas none of the patients with *APP* mutations exhibited spastic paraplegia. Epilepsy/seizure was described in 8% of patients with *PSEN1* and 6% of patients with *APP* mutations,

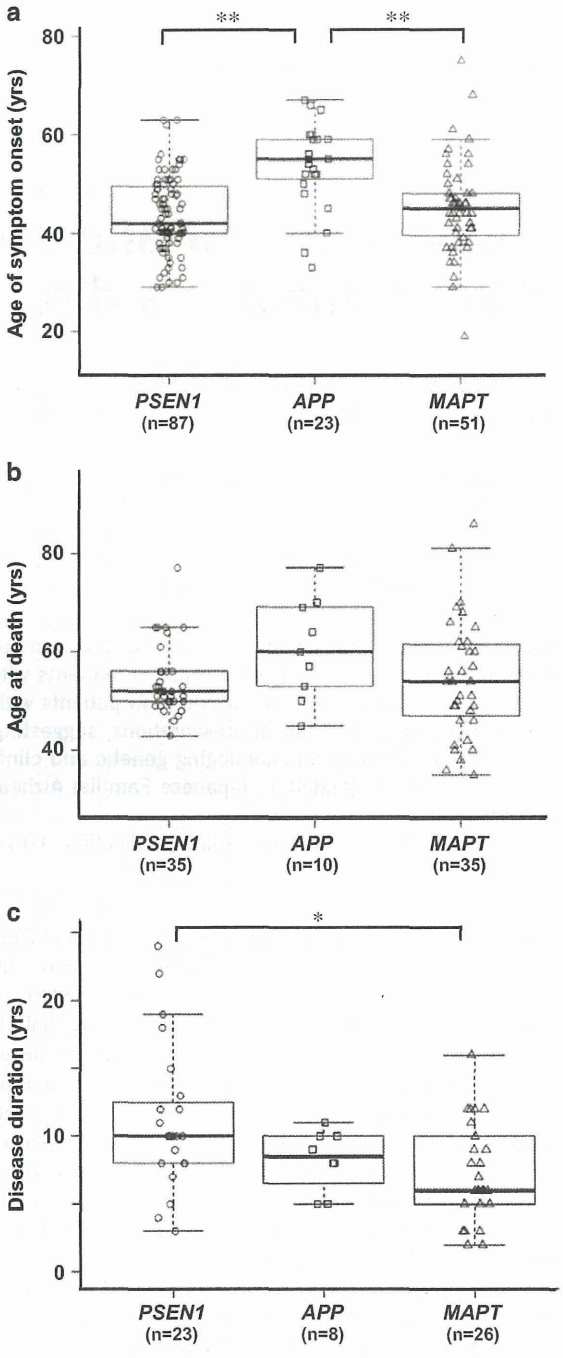

Figure 1 Age at onset and death, and disease duration in Japanese FAD and FTDP-17 patients. (**a**) Age at onset for patients grouped on the basis of *PSEN1*, *APP* and *MAPT* mutations. The horizontal line in the box indicates the median, the lower and upper boundaries of the box represent the lower and upper quartile boundaries, respectively, and whiskers are 1.5 times the interquartile range. Patients with *PSEN1* and *MAPT* mutation showed significantly younger age at onset than patients with *APP* mutations (**$P<0.01$, ANOVA with *post hoc* Tukey's test). (**b**) Age at death of three groups with gene mutations. There was no significant difference in age at death among the groups. (**c**) Disease duration was defined as the period from age at onset to death. The disease courses of patients with *MAPT* mutations (7 ± 4 years, mean $\pm$ s.d.) were significantly shorter than those with *PSEN1* mutations (11 ± 5) (*$P<0.05$, ANOVA with *post hoc* Tukey's test). ANOVA, analysis of variance; FAD, familial Alzheimer's disease; FTDP-17, frontotemporal dementia with parkinsonism linked to chromosome 17.

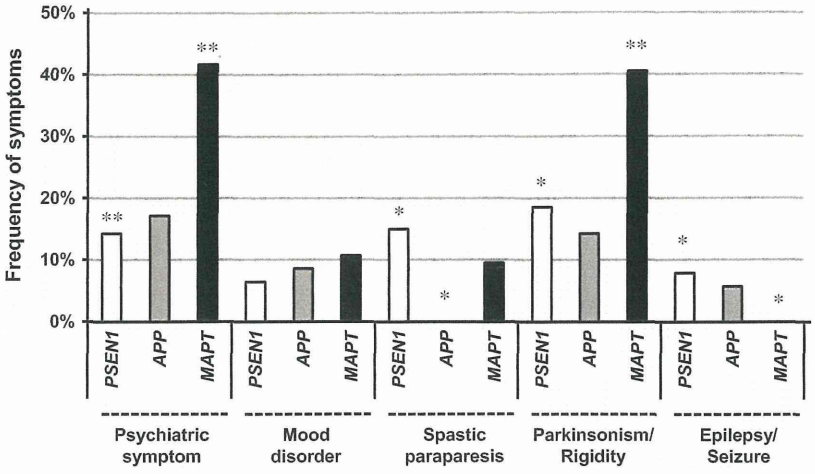

Figure 2 Frequency of each clinical manifestation in patients with Japanese FAD and FTDP-17. We investigated the presence or absence of psychiatric symptoms, mood disorders, spastic paraplegia, parkinsonism and epilepsy/seizure by careful reading of the original papers. We determined the frequency of each of the clinical manifestations by counting the number of patients for whom the presence of the manifestation was described in literature. In case there was no description of the manifestation, the patient was not counted as manifesting the manifestation. The observed frequencies of causative gene mutation were significantly different from the expected frequencies determined by residual analyses for χ^2 statistical analysis (*$P<0.05$, **$P<0.01$). FAD, familial Alzheimer's disease; FTDP-17, frontotemporal dementia with parkinsonism linked to chromosome 17.

whereas none of the patients with *MAPT* mutations exhibited epilepsy/seizure. Previous studies showed that the frequency of seizure was relatively high in patients with early onset of AD,[13,14] and low in patients with *MAPT* mutations.[15] These findings suggest that epilepsy/seizure is closely associated with amyloid pathology, and that tauopathy alone may not be sufficient to cause epilepsy. Taken together, mutations in causative genes may modify the clinical presentations in patients with familial dementia.

In summary, we have comprehensively collected, cataloged and systematically meta-analyzed the data from currently available data on Japanese FAD and FTDP-17. We made all the results publicly available on the online database 'JFADdb'. The database may provide information useful for estimating the age at onset and the natural course of disease in future preventive or therapeutic trials of Japanese FAD.

CONFLICT OF INTEREST

The authors declare no conflict of interest.

ACKNOWLEDGEMENTS

This work is supported in part by Grants-in-Aid for scientific research from Japan Society of Promotion of Science, Japan (26870209 to KK, 23591234 and 20372469 to TI) and Grant-in-Aid from the Ministry of Health, Labour and Welfare of Japan. We are grateful to Dr Hasegawa and Ms Fukaumi for their technical assistance.

1 Karch, C. M., Cruchaga, C. & Goate, A. M. Alzheimer's disease genetics: from the bench to the clinic. *Neuron* **83**, 11–26 (2014).
2 Guerreiro, R. J., Gustafson, D. R. & Hardy, J. The genetic architecture of Alzheimer's disease: beyond APP, PSENs and APOE. *Neurobiol. Aging* **33**, 437–456 (2012).
3 Rademakers, R., Dermaut, B., Peeters, K., Cruts, M., Heutink, P. & Goate, A. *et al.* Tau (MAPT) mutation Arg406Trp presenting clinically with Alzheimer disease does not share a common founder in Western Europe. *Hum. Mutat.* **22**, 409–411 (2003).
4 Ikeuchi, T., Kaneko, H., Miyashita, A., Nozaki, H., Kasuga, K. & Tsukie, T. *et al.* Mutational analysis in early-onset familial dementia in the Japanese population. The role of PSEN1 and MAPT R406W mutations. *Dement. Geriatr. Cogn. Disord.* **26**, 43–49 (2008).
5 Pruitt, K. D., Brown, G. R., Hiatt, S. M., Thibaud-Nissen, F., Astashyn, A. & Ermolaeva, O. *et al.* RefSeq: an update on mammalian reference sequences. *Nucleic Acids Res.* **42**, D756–D763 (2014).
6 Cruts, M., Theuns, J. & Van Broeckhoven, C. Locus-specific mutation databases for neurodegenerative brain diseases. *Hum. Mutat.* **33**, 1340–1344 (2012).
7 Tomiyama, T., Nagata, T., Shimada, H., Teraoka, R., Fukushima, A. & Kanemitsu, H. *et al.* A new amyloid beta variant favoring oligomerization in Alzheimer's-type dementia. *Ann. Neurol.* **63**, 377–387 (2008).
8 Ogaki, K., Li, Y., Takanashi, M., Ishikawa, K., Kobayashi, T. & Nonaka, T. *et al.* Analyses of the MAPT, PGRN, and C9orf72 mutations in Japanese patients with FTLD, PSP, and CBS. *Parkinsonism Relat. Disord.* **19**, 15–20 (2013).
9 Ryman, D. C., Acosta-Baena, N., Aisen, P. S., Bird, T., Danek, A. & Fox, N. C. *et al.* Symptom onset in autosomal dominant Alzheimer disease: a systematic review and meta-analysis. *Neurology* **83**, 253–260 (2014).
10 Foster, N. L., Wilhelmsen, K., Sima, A. A. F., Jones, M. Z. & D'Amato, C. J. *et al.* Frontotemporal dementia and parkinsonism linked to chromosome 17: a consensus conference. *Ann. Neurol.* **41**, 706–715 (1997).
11 Larner, A. J. & Doran, M. Clinical phenotypic heterogeneity of Alzheimer's disease associated with mutations of the presenilin-1 gene. *J. Neurol.* **253**, 139–158 (2006).
12 Tabira, T., Chui, D. H., Nakayama, H., Kuroda, S. & Shibuya, M. Alzheimer's disease with spastic paresis and cotton wool type plaques. *J. Neurosci. Res.* **70**, 367–372 (2002).
13 Noebels, J. A perfect storm: converging paths of epilepsy and Alzheimer's dementia intersect in the hippocampal formation. *Epilepsia* **52**, 39–46 (2011)
14 Vossel, K. A., Beagle, A. J., Rabinovici, G. D., Shu, H., Lee, S. E. & Naasan, G. *et al.* Seizures and epileptiform activity in the early stages of Alzheimer disease. *JAMA Neurol.* **70**, 1158–1166 (2013).
15 Sperfeld, A. D., Collatz, M. B., Baier, H., Palmbach, M., Storch, A. & Schwarz, J. *et al.* FTDP-17: an early-onset phenotype with parkinsonism and epileptic seizures caused by a novel mutation. *Ann. Neurol.* **46**, 708–715 (1999).

Supplementary Information accompanies the paper on Journal of Human Genetics website (http://www.nature.com/jhg)

Biochemical and Biophysical Research Communications 456 (2015) 482–488

Contents lists available at ScienceDirect

Biochemical and Biophysical Research Communications

journal homepage: www.elsevier.com/locate/ybbrc

ApoE-isoform-dependent cellular uptake of amyloid-β is mediated by lipoprotein receptor LR11/SorLA

Ryuji Yajima [a], Takayoshi Tokutake [a], Akihide Koyama [b], Kensaku Kasuga [a,b,c], Toshiyuki Tezuka [a,c], Masatoyo Nishizawa [a], Takeshi Ikeuchi [c,*]

[a] Department of Neurology, Brain Research Institute, Niigata University, Niigata, Japan
[b] Center for Transdisciplinary Research, Niigata University, Niigata, Japan
[c] Department of Molecular Genetics, Brain Research Institute, Niigata University, Niigata, Japan

ARTICLE INFO

Article history:
Received 7 November 2014
Available online 5 December 2014

Keywords:
Alzheimer's disease
LR11/SorLA
β-Amyloid
Apolipoprotein E

ABSTRACT

The formation of senile plaques composed of β-amyloid (Aβ) in the brain is likely the initial event in Alzheimer's disease (AD). Possession of the *APOE* ε4 allele, the strong genetic factor for AD, facilitates the Aβ deposition from the presymptomatic stage of AD in a gene-dosage-dependent manner. However, the precise mechanism by which apoE isoforms differentially induce the AD pathology is largely unknown. LR11/SorLA is a type I membrane protein that functions as the neuronal lipoprotein endocytic receptor of apoE and the sorting receptor of the amyloid precursor protein (APP) to regulate amyloidogenesis. Recently, LR11/SorLA has been reported to be involved in the lysosomal targeting of extracellular amyloid-β (Aβ) through the binding of Aβ to the vacuolar protein sorting 10 (VPS10) protein domain of LR11/SorLA. Here, we attempted to examine the human-apoE-isoform-dependent effect on the cellular uptake of Aβ through the formation of a complex between an apoE isoform and LR11/SorLA. Cell culture experiments using Neuro2a cells revealed that the cellular uptake of secreted apoE3 and apoE4 was enhanced by the overexpression of LR11/SorLA. In contrast, the cellular uptake of apoE2 was not affected by the expression of LR11/SorLA. Co-immunoprecipitation assay revealed that apoE-isoform-dependent differences were observed in the formation of an apoE-LR11 complex (apoE4 > apoE3 > apoE2). ApoE-isoform-dependent differences in cellular uptake of FAM-labeled Aβ were further investigated by coculture assay in which donor cells secrete one of the apoE isoforms and recipient cells express FL-LR11. The cellular uptake of extracellular Aβ into the recipient cells was most prominently accentuated when cocultured with the donor cells secreting apoE4 in the medium, followed by apoE3 and apoE2. Taken together, our results provide evidence for the mechanism whereby human-apoE-isoform-dependent differences modulate the cellular uptake of Aβ mediated by LR11/SorLA.

1. Introduction

Alzheimer's disease (AD) has emerged as the most prevalent form of dementia in adults. The cardinal pathological features of AD brain are the loss of synapses and neurons as well as abnormal accumulation of misfolded proteins such as β-amyloid (Aβ) and phosphorylated tau. The deposition of Aβ in the brain is considered to be the earliest event in AD [1] and is substantially affected by the *APOE* genotype, which has been shown to be a strong genetic risk factor for AD in various ethnic populations [2,3]. The presence of the *APOE* ε4 allele markedly increases the risk of developing AD and decreases the age at onset by 10 to 15 years; in contrast, the ε2 allele confers protection against AD development [4,5]. Although there have been numerous studies attempting to elucidate the mechanism underlying the increase or decrease in the risk of AD posed by different apoE isoforms [6], the exact mechanisms are still not completely understood. Thus, to address the differential effects of apoE isoforms on the amyloid pathology and Aβ metabolism is important in the elucidation of the AD pathogenic pathway.

LR11, also known as SorLA, is a type I membrane protein that has homology to members of the LDL receptor family and vacuolar

Abbreviations: AD, Alzheimer's disease; Aβ, amyloid-β; APP, amyloid precursor protein; VPS10, vacuolar protein sorting 10; TACE, tumor necrosis factor-α-converting enzyme; FL, full-length; CSF, cerebrospinal fluid; PCR, polymerase chain reaction; GFP, green fluorescent protein; HEK, human embryonic kidney; SDS–PAGE, sodium dodecyl sulfate–polyacrylamide gel electrophoresis; co-IP, coimmunoprecipitation.

* Corresponding author at: Department of Molecular Genetics, Brain Research Institute, Niigata University, 1-757 Asahimachi, Niigata 951-8585, Japan. Fax: +81 25 227 0793.
E-mail address: ikeuchi@bri.niigata-u.ac.jp (T. Ikeuchi).

http://dx.doi.org/10.1016/j.bbrc.2014.11.111
0006-291X/

protein sorting 10 (VPS10) protein family. LR11/SorLA is predominantly expressed on neurons in the cerebral cortex and hippocampus [7]. Reduced expression of LR11/SorLA in the brains of AD patients and subjects with mild cognitive impairment has been reported [8]. Furthermore, Aβ deposition is more prominent in *LR*11 knockout mice crossed with a mouse AD model [9]. These findings suggest the protective role of LR11/SorLA against AD pathology. In addition, some of the single-nucleotide polymorphisms (SNPs) in *SORL*1 encoding LR11/SorLA were found to be associated with a risk of sporadic AD in various ethnic backgrounds [3]. Full-length (FL) LR11/SorLA is cleaved by tumor necrosis factor-α-converting enzyme (TACE) to generate soluble LR11 [10]. We previously reported that the level of soluble LR11/SorLA was significantly high in the cerebrospinal fluid (CSF) of patients with AD [11]. The *APOE* ε4 carriers among AD patients showed higher levels of soluble LR11/SorLA than the ε4 noncarriers [11]. This suggests that the level of soluble LR11/SorLA in CSF is associated with AD in an apoE-isoform-dependent manner.

LR11/SorLA functions as the neuronal lipoprotein endocytic receptor of ApoE [12] and the sorting receptor of the amyloid precursor protein (APP) to regulate amyloidogenesis in endosomal and Golgi compartments [13]. LR11/SorLA interacts with newly synthesized APP in the Golgi apparatus and prevents the trafficking of APP into the cellular compartment where secretases reside. Consequently, the overexpression of LR11/SorLA in cultured cells reduces amyloidogenic processing [14]. Very recently, a novel function of LR11/SorLA has been reported. Caglayan et al. reported that LR11/SorLA plays a role in the lysosomal targeting of newly generated Aβ through the binding of Aβ to the amino-terminal VPS10 protein domain of LR11 [15]. This binding enhances Aβ clearance in lysosomes by internalization of extracellular Aβ through the receptor LR11/SorLA. With this as a background, we here attempted to determine the apoE-isoform-dependent effects on the cellular uptake of Aβ through the formation of a complex between an spoE isoform and LR11/SorLA.

2. Materials and methods

2.1. cDNA cloning and construction of expression plasmids

Complementary DNA (cDNA) of human full-length LR11 was amplified by PCR using pCMV6 plasmid cDNA containing human LR11 (Origene, Rockville, USA) and cloned into the pcDNA3.1 vector (Life Technologies, Carlsbad, USA). Human *APOE* ε3 cDNA was cloned and inserted into the pcDNA3.1 vector. We generated two allelic variants of human *APOE*, namely, *APOE* ε2 and ε4, by mutagenesis. Each isoform of *APOE* was cloned into the pEGFP vector (Clontech, Mountain View, USA). All constructs generated from PCR products were verified by DNA sequencing.

2.2. Cell culture and transfection

Mouse neuroblastoma Neuro2a (N2a) and human embryonic kidney (HEK)293T cells were cultured as previously described [16]. Transient transfection of plasmid DNA into cells was carried out by using Lipofectamine 2000 (Life Technologies). To generate stable cell lines, N2a cells transfected with cDNA encoding human apoE2, apoE3, apoE4 or FL-LR11 were selected using G418. Peptides of Aβ40 were purchased from Wako (Tokyo, Japan) and FAM-labeled Aβ40 from AnaSpec (Fremont, USA). They were dissolved in 1% ammonium hydroxide.

2.3. Coculture system

Coculture experiments were performed essentially as previously described [16]. Donor HEK293T cells transiently transfected with cDNA encoding human apoE2, apoE3, apoE4, apoE2-GFP, apoE3-GFP, or apoE4-GFP were cultured on a dish with a 1.0 μm filter insert (BD Bioscience, San Diego, USA) for 24 h. The donor HEK293T cells on the dish were placed in a six-well culture dish containing the recipient N2a cells mock-transfected or transiently transfected with the FL-LR11 cDNA construct. After 24 h of coculture, the lysate of the recipient cells and the medium were subjected to Western blot analysis.

2.4. Western blot analysis

The cells were solubilized using a lysis buffer (150 mM NaCl, 50 mM Tris-HCl, pH 7.4, 0.5% NP-40, 0.5% sodium deoxycholate, and 5 mM EDTA). The protein concentration of the detergent-extracted lysates was determined using a bicinchoninic acid protein assay kit (Pierce, Rockford, USA). Equal amounts of protein were boiled in Laemmli sample buffer and then subjected to Tris–glycine or Tris-tricine SDS–PAGE system. The separated proteins were transferred to a polyvinylidene difluoride membrane (Millipore, Billerica, USA) and then incubated with appropriate primary antibodies. FL-LR11 and sLR11 were detected using the monoclonal antibody 48/LR11 (BD Biosciences), which recognizes the extracellular domain of LR11. ApoE was visualized by the monoclonal antibody E6D7 (Sigma, St. Louis, USA). Aβ polypeptides were detected by the monoclonal antibody 6E10 (Covance, Berkeley, USA). GFP-fusion proteins were detected by the monoclonal antibody1E4 (MBL, Japan). Actin was detected using the goat anti-actin antibody I-19 (Santa Cruz Biotechnology, Dallas, USA). Immunoreactive bands were detected using an Immobilon Western Chemiluminescent HRP substrate (Millipore). The band intensities were quantified using a LAS system (GE Healthcare, Pittsburgh, USA).

2.5. Co-immunoprecipitation assays

HEK293T cells were cotransfected with the cDNA encoding apoE2, apoE3, or apoE4 and with FL-LR11 cDNA. The cells were solubilized using co-IP buffer (1% CHAPS, 150 mM NaCl, 50 mM HEPES, pH 7.5). The supernatant was incubated with either an anti-LR11 antibody (48/LR11) or an anti-apoE antibody (AB947, Millipore) at 4 °C for 16 h. To immunoprecipitate the protein complex, 25 μL of protein G Mag Sepharose beads (GE Healthcare) was added to the mixture, and the mixture was incubated on a rotator at 4 °C. The beads were collected on a magnetic stand and washed three times with the solubilization buffer. The immunoprecipitated proteins were released from the beads by incubation in Laemmli sample buffer. The obtained samples were analyzed by SDS–PAGE followed by Western blot analysis.

2.6. Fluorescence confocal laser scanning microscopy and image analysis

N2a cells treated with GFP-labeled apoE3 or FAM-labeled Aβ40 were cultured. All images were obtained using an inverted microscope (TE-300NT, Nikon, Japan) and a confocal microscope (CSU-10, Yokogawa Electric Corp, Japan). The obtained images were further analyzed with a quantitative analysis system (AquaCosmos, Hamamatsu Photonics, Japan).

2.7. Statistical analyses

Data are shown as the mean ± standard error of the mean (SEM). Statistical comparison between two groups was carried out by the Student *t*-test. For statistical comparison among several groups, we used one-way analysis of variance (ANOVA) followed

by the Tukey post hoc test. The statistical analyses were performed using SPSS ver. 12.0 J (SPSS Japan).

3. Results

3.1. Isoform-dependent change in level of secreted apoE by expression of LR11/SorLA

We first determined whether the expression of FL-LR11/SorLA affects the levels of apoE in the lysate and medium. N2a cells stably expressing human apoE3 were mock-transfected or transiently transfected with human FL-LR11 cDNA. The levels of apoE3 in the medium and lysate were determined using the anti-apoE antibody at different time points from 2 to 24 h after the medium was replaced. The level of apoE3 migrating at ~34 kDa and secreted into the medium increased after the medium replacement in a time-dependent manner (Fig. 1A). The level of apoE3 in the medium was significantly lower in N2a cells transfected with FL-LR11 24 h after the medium change compared with mock-transfected cells, whereas the level of apoE in the lysate was comparable between the mock- and FL-LR11-transfected cells (Fig. 1B).

Next, we investigated whether apoE-isoform-dependent differences are observed in this study. N2a cells stably expressing human apoE2, apoE3, or apoE4, were mock-transfected or transiently transfected with FL-LR11, and the levels of apoE in the medium and lysate were determined by immunoblot analysis. The apoE ratio (medium/lysate) significantly decreased in apoE3- and E4-expressing cells that were transiently transfected with FL-LR11 (Fig. 1C and D), whereas the apoE ratio (medium/lysate) was unchanged in apoE2-expressing cells transfected with FL-LR11. These findings suggest that the effect of LR11/SorLA on apoE ratio (medium/lysate) is dependent on the apoE isoform.

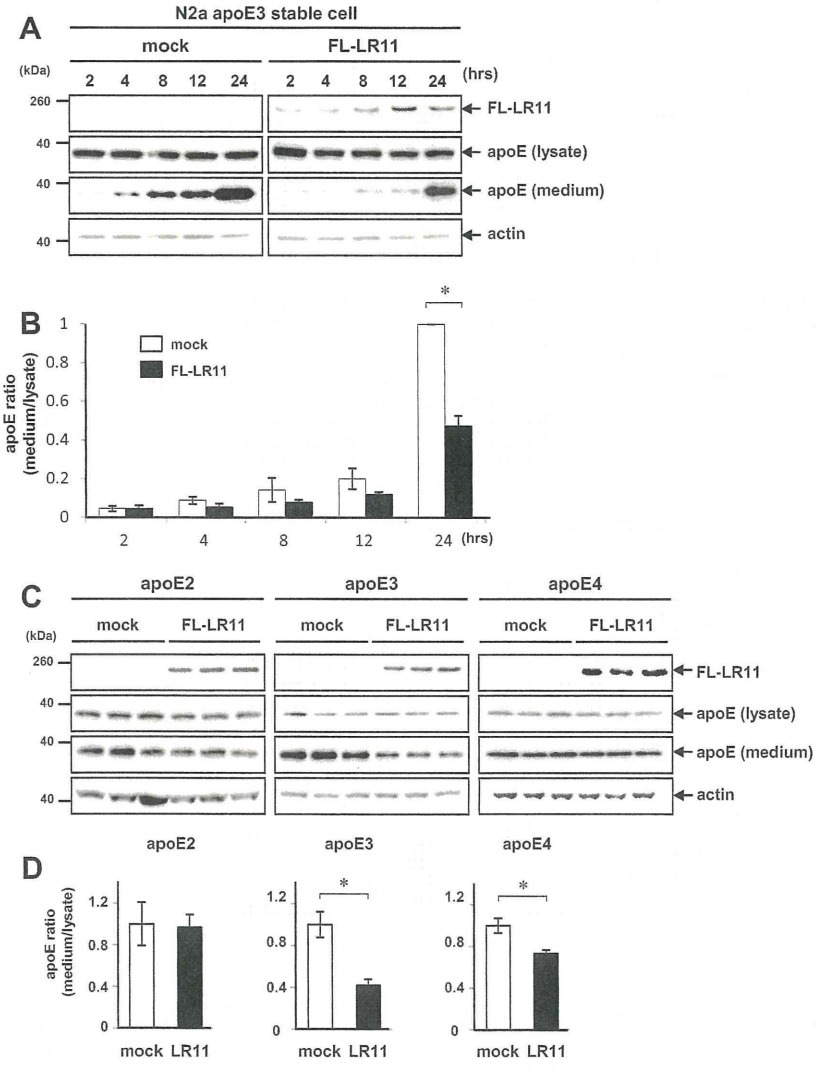

Fig. 1. Human-apoE-isoform-dependent differences in apoE ratio mediated by LR11/SorLA. (A) N2a cells stably expressing human apoE3 were mock-transfected or transiently transfected with human FL-LR11. The levels of apoE3 in the medium and cell lysate were determined by immunoblot analysis at different time points ranging from 2 to 24 h after the medium change. Note that the level of apoE in the medium of cells expressing FL-LR11 was decreased compared with mock-transfected cells. The equivalence of protein loading is shown in the β-actin blot. (B) Results of semiquantitative analysis by densitometry of apoE level. The apoE ratio (medium/lysate) was defined as the ratio of the level of apoE in the medium to that in the cell lysate. The apoE ratio (medium/lysate) significantly decreased 24 h after the medium change in cells transfected with FL-LR11 compared with mock-transfected cells. Results of three independent experiments are shown as mean ± SEM. *$p < 0.05$ by Student t-test. (C) N2a cells stably expressing human apoE2, apoE3, or apoE4 were mock-transfected or transiently transfected with human FL-LR11. The levels of apoE in the medium and the lysate of cells expressing each of the apoE isoforms were determined 24 h after the medium change. (D) Results of semiquantitative analysis of the apoE ratio (medium/lysate). The apoE ratio (medium/lysate) was significantly decreased in apoE3- or apoE4-expressing cells transfected with FL-LR11, whereas the apoE ratio did not change in apoE2-expressing cells. *$p < 0.05$.

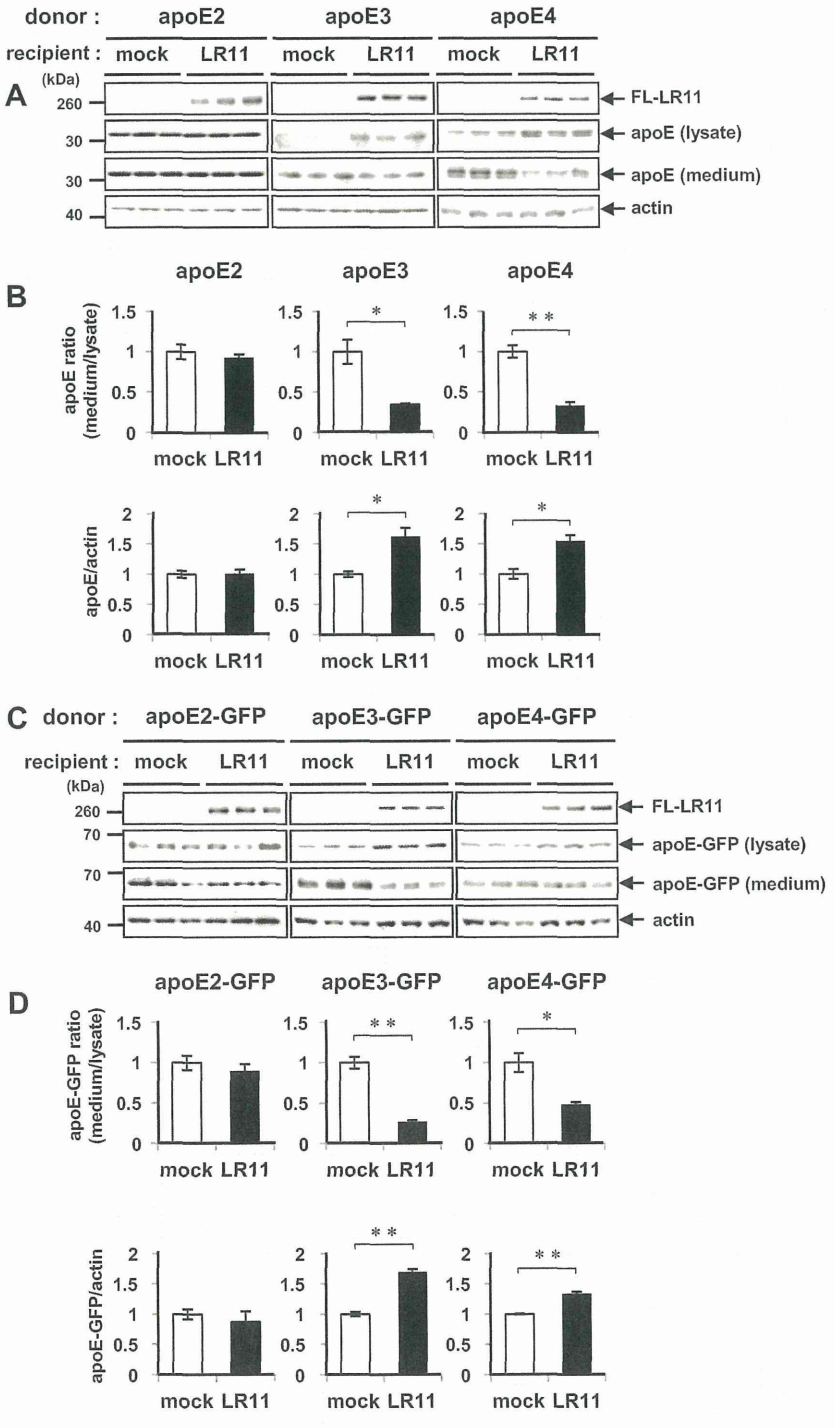

Fig. 2. ApoE isoform-dependent cellular uptake of apoE by LR11/SorLA in coculture system. (A) The recipient N2a cells mock-transfected or transiently transfected with FL-LR11 were cocultured with the donor HEK293T cells that were transiently transfected with apoE2, apoE3, or apoE4 for 24 h. Cellular uptake of secreted apoE from the medium into the recipient N2a cells was examined by Western blot analysis. (B) Results of semiquantitative analysis of cellular uptake of apoE are shown. The apoE ratio (medium/lysate) significantly decreased in the recipient cells transfected with FL-LR11 compared with the mock-transfected recipient cells when the recipient cells were cocultured with the donor HEK293T cells expressing apoE3 or apoE4 (*upper panels*). The apoE level normalized by β-actin level in the lysate of the recipient cells transfected with FL-LR11 showed a significant increase compared with that of mock-transfected recipient cells when the recipient cells were cocultured with the donor HEK293T cells expressing apoE3 or apoE4 (*lower panels*). $^{*}p < 0.05$; $^{**}p < 0.01$. (C) The recipient N2a cells mock-transfected or transiently transfected with FL-LR11 were cocultured with the donor HEK293T cells that secreted apoE2-GFP, apoE3-GFP, or apoE4-GFP in the medium for 24 h. Cellular uptake of apoE from the medium into the recipient N2a cells was examined. (D) Results of semiquantitative analysis of cellular uptake of apoE-GFP are shown. The apoE ratios (medium/lysate) for the apoE isoforms are shown (*upper panels*). The levels of apoE-GFP normalized by β-actin level for the apoE isoforms are shown (*lower panels*). $^{*}p < 0.05$; $^{**}p < 0.01$.

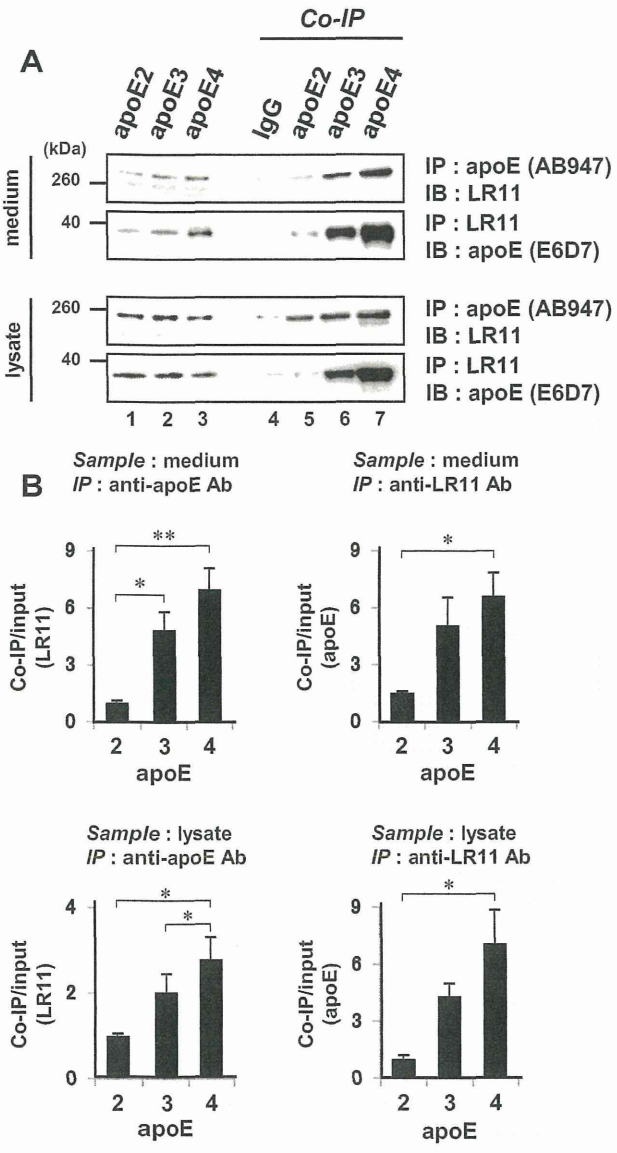

Fig. 3. Human-apoE-isoform-dependent differences in formation of complex between apoE and LR11/SorLA examined by co-IP assay. (A) HEK293T cells were cotransfected with each of the human apoE isoforms and human FL-LR11. The formed complex between apoE and LR11/SorLA was immunoprecipitated using the anti-apoE antibody (AB947) or anti-LR11 antibody (48/LR11), followed by immunoblot analysis. The lysates (*lanes* 1–3) and immunoprecipitated samples (*lanes* 4–7) were run on the same gel. (B) Results of semiquantitative analysis of immunoprecipitated apoE and LR11/SorLA. $^{*}p < 0.05$; $^{**}p < 0.01$ by Tukey test following ANOVA.

3.2. Cellular uptake of apoE examined by fluorescence confocal laser microscopy

The finding that the level of apoE in the medium of cells transfected with FL-LR11 decreased raises the possibility that apoE in the medium was taken up into cells by the lipoprotein receptor LR11/SorLA. To explore this possibility, N2a cells were incubated with the medium prepared from cells that transiently expressed the apoE3-GFP fusion protein. Fluorescence confocal microscopy revealed apoE-GFP signals inside the cells transfected with FL-LR11 and incubated with the medium of cells expressing apoE3-GFP (Supplementary Fig. 1B). This finding suggests that the cellular uptake of apoE from the medium was enhanced by the expression of LR11/SorLA.

3.3. ApoE-isoform-dependent cellular uptake of apoE in coculture system

We next examined whether the enhanced uptake of apoE by FL-LR11 is modified by apoE isoforms using the coculture system. First, we attempted to confirm whether apoE3 and GFP-labeled apoE3 secreted from the donor HEK293T cells are taken up into the recipient cells. This experiment revealed that apoE3 and GFP-labeled apoE3 were detected in the lysate of the recipient cells (Supplementary Fig. 2B), whereas GFP alone without apoE was not detected in the recipient cells.

Having established that apoE secreted from the donor cells is taken up into the recipient cells, we next asked if isoforms of apoE differently affect the cellular uptake of apoE in the recipient N2a cells mock-transfected or transiently transfected with FL-LR11. The level of apoE taken up into the recipient N2a cells was determined by immunoblot analysis using the anti-apoE antibody (Fig. 2A). The cellular uptake levels of apoE3 and apoE4 were significantly higher in the recipient cells that express FL-LR11 compared with the mock-transfected cells (Fig. 2B). In a similar experiment using donor cells that express apoE2-GFP, apoE3-GFP, or apoE4-GFP, the cellular uptake levels of apoE3-GFP and apoE4-GFP were increased by the expression of FL-LR11 (Fig. 2C and D). These results suggest that FL-LR11 enhances the cellular uptake of apoE3 and apoE4 but not that of apoE2.

3.4. ApoE-isoform-dependent binding affinity to LR11/SorLA

We speculated that the differential cellular apoE uptake in the recipient cells may be explained by a difference in binding affinity between LR11/SorLA and each of the apoE isoforms. To test this hypothesis, we examined the ability of LR11/SorLA to form a complex with each of the apoE isoforms by co-immunoprecipitation (co-IP) assay. We collected the detergent-extracted lysate of HEK293T cells that were cotransfected with FL-LR11 and each of the apoE isoforms. Co-IP assay using the anti-apoE or anti-LR11 antibody was performed using the medium and cell lysate. This assay revealed that LR11/SorLA bound to each isoform of apoE with different efficiencies (Fig. 3A). ApoE4-expressing cells showed the highest level of the LR11-apoE complex, followed by apoE3- and apoE2-expressing cells (Fig. 3B).

3.5. ApoE-isoform-dependent cellular uptake of Aβ

Given the physical interaction between LR11/SorLA and apoE, we next considered the possibility that FL-LR11 may be involved in the cellular uptake of the apoE-Aβ complex, because apoE is known to form a complex with Aβ. To address this issue, N2a cells were incubated with FAM-labeled Aβ40 at various concentrations of ranging from 0.5 to 3.0 μM. By fluorescence confocal laser microscopy, we detected the cellular uptake of FAM-labeled Aβ at concentrations above 1.0 μM (Supplementary Fig. 3A). We observed the cellular uptake of FAM-labeled Aβ at a low concentration of 0.25 μM when the recipient cells were transfected with FL-LR11 and cocultured with the donor cells expressing apoE4 (Supplementary Figs. 3B, 4A and 4B). The finding suggests that the cellular uptake of Aβ was enhanced in the presence of both FL-LR11 and apoE.

We finally performed coculture experiments in which the recipient N2a cells mock-transfected or transiently transfected with FL-LR11 were cocultured with the donor cells expressing apoE2, E3, or E4 in the presence of the Aβ peptides at 0.25 μM. The cellular uptake level of apoE and Aβ were highest when the recipient cells were cocultured with the donor cells expressing apoE4, followed by apoE3 and apoE2 (Fig. 4A and B).

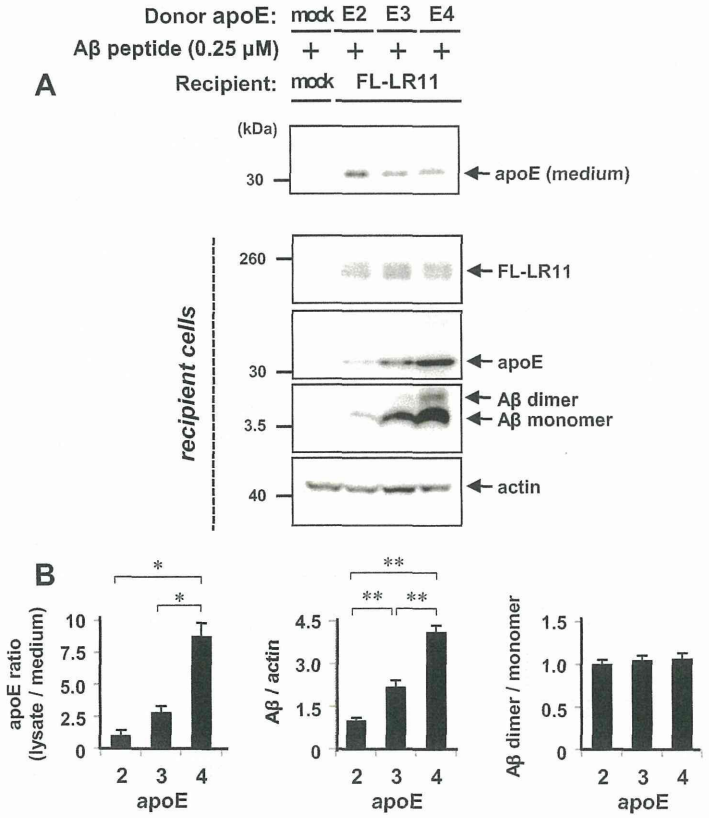

Fig. 4. ApoE-isoform-dependent differences in cellular uptake of Aβ in cells expressing LR11/SorLA. (A) Recipient N2a cells stably expressing human FL-LR11 were cocultured with donor N2a cells stably expressing human apoE2, apoE3, or apoE4 in the presence of Aβ40 peptides at 0.25 μM for 24 h. The cellular uptake of Aβ and apoE into the recipient cells was examined by Western blot analysis. (B) Results of semiquantitative analysis of cellular uptake of Aβ and apoE are shown as -fold increase compared with the apoE2 isoform. $^{*}p < 0.05$; $^{**}p < 0.01$ by Tukey test following ANOVA.

4. Discussion

Despite significant advances in our understanding of the pathological events occurring in the AD brain, the factors leading to Aβ accumulation in sporadic AD patients are not well understood. A wealth of evidence has confirmed that *APOE* ε4 is the strongest genetic risk factor for sporadic AD [2,3]. Although it is not fully understood how human apoE isoforms differentially affect the various pathogenic processes implicated in AD, several lines of evidence suggest that the effects of apoE on Aβ accumulation, aggregation, clearance, neurotoxicity, and neuroinflammation may play a role in AD pathogenesis [6]. Hence, understanding how each of the apoE isoforms differentially plays a pathophysiological role in AD is an important question to address. In this regard, this study provided new insights into how apoE isoforms differentially modify the AD pathogenic pathway with particular focus on the cellular uptake of Aβ via the lipoprotein receptor LR11/SorLA.

First, we demonstrated that the overexpression of LR11/SorLA enhanced the cellular uptake of apoE3 and apoE4. This finding suggests that LR11/SorLA functions as the apoE receptor. This notion was suggested by previous studies showing that FL-LR11 at the cell surface was capable of cellular uptake of apoE [12]. Importantly, we here showed that the cellular uptake of apoE is modified by different apoE isoforms. The cellular uptake of apoE4 and apoE3 was significantly enhanced by the expression of LR11/SorLA. In support of this notion, the co-IP assay revealed that the apoE-LR11/SorLA complex formation showed apoE-isoform-dependent differences in efficiencies, that is, apoE4 > apoE3 > apoE2. Major apoE receptors belong to the LDL receptor family including the LDL receptor and LDLR-related protein (LRP1). Different efficiencies in the formation of complexes between the LDL receptor and the apoE isoforms were observed. Similar to our finding, the cellular uptake levels of apoE3 and apoE4 were previously found to be higher than that of apoE2 in cells expressing the LDL receptor [17].

Secondly, our cell culture experiments revealed that extracellular Aβ was taken up into cells overexpressing LR11/SorLA in an apoE-isoform-dependent manner. A recent study has shown that LR11/SorLA binds to Aβ directly through the VPS10 protein domain of LR11/SorLA [15]. Importantly, we demonstrated that the cellular uptake of extracellular Aβ was apoE-isoform-dependent, that is, apoE4 > apoE3 > apoE2. Although this finding is potentially interesting, how this finding is relevant to AD pathogenesis is not presently understood. Enhancement of cellular uptake of Aβ may have two different consequences. A harmful consequence would be that an increased intracellular Aβ concentration through the uptake of extracellular Aβ may provide seeds of Aβ oligomers, a toxic forms of Aβ [18]. Some studies suggested that intracellular Aβ oligomers may be a major cause of synaptic dysfunction [19]. On the other hand, a beneficial consequence would be that the cellular uptake of extracellular Aβ may enhance the clearance of Aβ in lysosomes [20]. Our finding favors the former possibility, that is, cellular uptake of Aβ may exert a detrimental effect on neurons because this phenomenon is most closely associated with the presence of apoE4. Further studies delineating the precise consequences of increased intracellular Aβ level caused by enhanced cellular uptake of Aβ will be required.

ApoE is predominantly generated by astrocytes and microglia in the brain and is subsequently lipidated by ABCA1 to form lipoprotein particles [21]. It has been demonstrated that lipoprotein receptors including LDLR and LRP on the neuronal surface are able to take apoE-Aβ complexes into neurons after apoE is lipidated [22]. The lipidation of apoE has been shown to influence its isoform-specific affinity to Aβ. The efficiency of complex formation between lipidated apoE and Aβ is in the order of apoE2 > apoE3 > apoE4 [23]. In addition, the variable levels of apoE oxidation may affect the properties of apoE binding to Aβ. In this study, we did not fully address the lipidation or oxidation status of apoE secreted from HEK293T cells, which should be taken into account when interpreting our results. To minimize confounding factors, it is desirable to use apoE prepared under conditions that preserve apoE lipidation and oxidation status found in the brain. Collectively, our study indicated that LR11/SorLA is capable of cellular uptake of Aβ in an apoE-isoform-dependent manner; however, its pathophysiological role requires further investigation.

Acknowledgments

This work is supported in part by JSPS KAKENHI (23591234 and 20372469 to T.I.) and a Grant-in-Aid from the Ministry of Health, Labour and Welfare of Japan.

Appendix A. Supplementary data

Supplementary data associated with this article can be found, in the online version, at http://dx.doi.org/10.1016/j.bbrc.2014.11.111.

References

[1] C.R. Jack, D.M. Holtzman, Biomarker modeling of Alzheimer's disease, Neuron 80 (2013) 1347–1358.
[2] J.C. Lambert, C.A. Ibrahim-Verbaas, D. Harold, et al., Meta-analysis of 74,046 individuals identifies 11 new susceptibility loci for Alzheimer's disease, Nat. Genet. 45 (2013) 1452–1458.
[3] A. Miyashita, A. Koike, G. Jun, et al., SORL1 is genetically associated with late-onset Alzheimer's disease in Japanese, Koreans and Caucasians, PLoS One 8 (2013) e58618.
[4] E.H. Corder, A.M. Saunders, W.J. Strittmatter, et al., Gene dose of apolipoprotein E type 4 allele and the risk of Alzheimer's disease in late onset families, Science 261 (1993) 921–923.
[5] E.H. Corder, A.M. Saunders, N.J. Risch, et al., Protective effect of apolipoprotein E type 2 allele for late onset Alzheimer disease, Nat. Genet. 7 (1994) 180–184.
[6] C.C. Liu, T. Kanekiyo, H. Xu, et al., Apolipoprotein E and Alzheimer disease: risk, mechanisms and therapy, Nat. Rev. Neurol. 9 (2013) 106–118.
[7] Y. Motoi, T. Aizawa, S. Haga, et al., Neuronal localization of a novel mosaic apolipoprotein E receptor, LR11, in rat and human brain, Brain Res. 833 (1999) 209–215.
[8] K.L. Sager, J. Wuu, S.E. Leurgans, et al., Neuronal LR11/SorLA expression is reduced in mild cognitive impairment, Ann. Neurol. 62 (2007) 640–647.
[9] S.E. Dodson, O.M. Andersen, V. Karmali, et al., Loss of LR11/SorLA enhances early pathology in a mouse model of amyloidosis: evidence for a proximal role in Alzheimer's disease, J. Neurosci. 28 (2008) 12877–12886.
[10] M. Jiang, H. Bujo, K. Ohwaki, et al., Ang II-stimulated migration of vascular smooth muscle cells is dependent on LR11 in mice, J. Clin. Invest. 118 (2008) 2733–2746.
[11] T. Ikeuchi, S. Hirayama, T. Miida, et al., Increased levels of soluble LR11 in cerebrospinal fluid of patients with Alzheimer disease, Dement. Geriatr. Cogn. Disord. 30 (2010) 28–32.
[12] H. Yamazaki, H. Bujo, J. Kusunoki, et al., Elements of neural adhesion molecules and a yeast vacuolar protein sorting receptor are present in a novel mammalian low density lipoprotein receptor family member, J. Biol. Chem. 271 (1996) 24761–24768.
[13] O.M. Andersen, J. Reiche, V. Schmidt, et al., Neuronal sorting protein-related receptor SorLA/LR11 regulates processing of the amyloid precursor protein, Proc. Natl. Acad. Sci. U.S.A. 102 (2005) 13461–13466.
[14] A. Schmidt, M. Sporbert, M. Rohe, et al., SorLA/LR11 regulates processing of amyloid precursor protein via interaction with adaptors GGA and PACS-1, J. Biol. Chem. 282 (2007) 32956–32964.
[15] S. Caglayan, S. Takagi-Niidome, F. Liao, et al., Lysosomal sorting of amyloid-β by the SorLA receptor is impaired by a familial Alzheimer's disease mutation, Sci. Transl. Med. 6 (2014). 223ra220.
[16] T. Tokutake, K. Kasuga, R. Yajima, et al., Hyperphosphorylation of Tau induced by naturally secreted amyloid-β at nanomolar concentrations is modulated by insulin-dependent Akt-GSK3β signaling pathway, J. Biol. Chem. 287 (2012) 35222–35233.
[17] T. Simmons, Y.M. Newhouse, K.S. Arnold, et al., Human low density lipoprotein receptor fragment. Successful refolding of a functionally active ligand-binding domain produced in *Escherichia coli*, J. Biol. Chem. 272 (1997) 25531–25536.
[18] X. Hu, S.L. Crick, G. Bu, et al., Amyloid seeds formed by cellular uptake, concentration, and aggregation of the amyloid-beta peptide, Proc. Natl. Acad. Sci. U.S.A. 106 (2009) 20324–20329.
[19] P.N. Lacor, M.C. Buniel, P.W. Furlow, et al., Aβ oligomer-induced aberrations in synapse composition, shape, and density provide a molecular basis for loss of connectivity in Alzheimer's disease, J. Neurosci. 27 (2007) 796–807.
[20] J. Li, T. Kanekiyo, M. Shinohara, et al., Differential regulation of amyloid-β endocytic trafficking and lysosomal degradation by apolipoprotein E isoforms, J. Biol. Chem. 287 (2012) 44593–44601.
[21] S.E. Wahrle, H. Jiang, M. Parsadanian, et al., Overexpression of ABCA1 reduces amyloid deposition in the PDAPP mouse model of Alzheimer disease, J. Clin. Invest. 118 (2008) 671–682.
[22] J. Kim, J.M. Basak, D.M. Holtzman, Overexpression of low-density lipoprotein receptor in the brain markedly inhibits amyloid deposition and increases extracellular Aβ clearance, Neuron 64 (2009) 632–644.
[23] T. Tokuda, M. Calero, E. Matsubara, et al., Lipidation of apolipoprotein E influences its isoform-specific interaction with Alzheimer's amyloid beta peptides, Biochem. J. 348 (2000) 359–365.

Globular Glial Mixed Four Repeat Tau and TDP-43 Proteinopathy with Motor Neuron Disease and Frontotemporal Dementia

Ryoko Takeuchi[1, 6]; Yasuko Toyoshima[1]; Mari Tada[1]; Hidetomo Tanaka[1]; Hiroshi Shimizu[1]; Atsushi Shiga[2]; Takeshi Miura[3]; Kenju Aoki[3]; Akane Aikawa[4]; Shin Ishizawa[4]; Takeshi Ikeuchi[5]; Masatoyo Nishizawa[6]; Akiyoshi Kakita[1]; Hitoshi Takahashi[1]

[1]Department of Pathology, Brain Research Institute, University of Niigata, Niigata, Japan

[2]Department of Molecular Neuroscience, Brain Research Institute, University of Niigata, Japan

[3]Department of Neurology, Toyama Prefectural Central Hospital, Toyama, Japan

[4]Department of Pathology, Toyama Prefectural Central Hospital, Toyama, Japan

[5]Department of Molecular Genetics, Brain Research Institute, University of Niigata, Niigata, Japan

[6]Department of Neurology, Brain Research Institute, University of Niigata, Niigata, Japan

Keywords

amyotrophic lateral sclerosis, astrocyte, frontotemporal lobar degeneration, motor neuron disease, tau, TDP-43

This article has been accepted for publication and undergone full peer review but has not been through the copyediting, typesetting, pagination and proofreading process, which may lead to differences between this version and the Version of Record. Please cite this article as doi: 10.1111/bpa.12262

Corresponding author:

Yasuko Toyoshima, MD, PhD, Department of Pathology, Brain Research Institute, University of Niigata, 1-757 Asahimachi, Chuo-ku, Niigata 951-8585, Japan (E-mail: *yasuko@bri.niigata-u.ac.jp*)

The authors declare no conflict of interest.

Abstract

Amyotrophic lateral sclerosis (ALS) may be accompanied by frontotemporal dementia (FTD). We report a case of glial mixed tau and TDP-43 proteinopathies in a Japanese patient diagnosed clinically as having ALS-D. Autopsy revealed loss of lower motor neurons and degeneration of the pyramidal tracts in the spinal cord and brainstem. The brain showed frontotemporal lobar degeneration (FTLD), the most severe neuronal loss and gliosis being evident in the precentral gyrus. Although less severe, such changes were also observed in other brain regions, including the basal ganglia and substantia nigra. AT8 immunostaining revealed that predominant occurrence of astrocytic tau lesions termed globular astrocytic inclusions (GAIs) was a feature of the affected regions. These GAIs were Gallyas-Braak-negative. Neuronal and oligodendrocytic tau lesions were comparatively scarce. pS409/410 immunostaining also revealed similar neuronal and glial TDP-43 lesions. Interestingly, occasional co-localization of tau and TDP-43 was evident in the GAIs. Immunoblot analyses revealed band patterns characteristic of a 4-repeat (4R) tauopathy, corticobasal degeneration and a TDP-43 proteinopathy, ALS/FTLD-TDP *Type B*. No mutations were found in the *MAPT* or *TDP-43* genes. We consider that this patient harbored a distinct, sporadic globular glial mixed 4R tau and TDP-43 proteinopathy associated with motor neuron disease and FTD. (199 words)

INTRODUCTION

Association of amyotrophic lateral sclerosis (ALS), the most common motor neuron disease (MND), with frontotemporal dementia (FTD) has been described (31, 35, 40). Since the discovery of a nuclear protein, TDP-43, as the pathological protein of frontotemporal lobar degeneration (FTLD) and ALS (4, 32), it has now been widely recognized that ALS (MND) and FTLD-TDP (dementia) are part of a spectrum of TDP-43 proteinopathy encompassing ALS at one end and FTLD-TDP at the other (16, 17). Some patients with ALS may have accompanying dementia (ALS-D) characterized by FTLD with TDP-43 pathology (33). On the other hand, some patients with FTLD-TDP may develop ALS during the disease course (FTLD-MND); TDP-43 pathology has been described in lower motor neurons in FTLD-TDP patients with, and even without, ALS (36).

The clinical picture of MND with FTD, or FTLD, may also be a feature in some tauopathies. We previously reported a sporadic 4-repeat (4R) tauopathy with FTLD, parkinsonism and MND in three Japanese patients, one with evident dementia; the most striking feature was the occurrence of unique astrocytic tau lesions (14, 34) different in morphology from tufted astrocytes (TAs) in progressive supranuclear palsy (PSP), or astrocytic plaques (APs) in corticobasal degeneration (CBD) (12). Recently, based on a compilation of cases of atypical tauopathies, including our above three cases (14, 34), a new category of 4R tauopathy designated globular glial tauopathies (GGT) has been proposed. These are characterized by tau-positive "globular" glial inclusions (GGIs) in oligodendrocytes (GOIs) and astrocytes (GAIs), and exhibit the clinical features of MND and/or FTD (1). Retrospectively, clinical diagnoses of PSP and CBD (or

corticobasal syndrome) are common in patients with GGT (1).

Here we report the neuropathological, biochemical and genetic findings in a case characterized by the occurrence of globular astrocytic tau and TDP-43 inclusions in a Japanese patient diagnosed clinically as having ALS-D.

PATIENT AND METHODS

The present study was conducted within the frame of a project, "Neuropathological and Molecular-Genetic Investigation of CNS Degenerative Diseases", approved by the Institutional Review Board of the University of Niigata. Informed consent was obtained from the patient's family prior to genetic analyses.

Case report

A 76-year-old Japanese woman became aware of gait disturbance, and subsequently developed dysarthria. On examination, she showed atrophy and fasciculation in the tongue, a hypoactive gag reflex, and muscle weakness in the upper extremities. Increased deep tendon reflexes were also present in the upper and lower extremities, with positive Babinski sign in both legs. About 10 months after onset, at the age of 77, she was diagnosed as having ALS.

Over the following year, she developed difficulty in swallowing and underwent gastrostomy for tube feeding. Her mental performance deteriorated rapidly and a state of apathy ensued; at this stage, the clinical diagnosis of ALS-D was made. She also suffered from progressive respiratory distress and underwent tracheotomy for artificial

respiratory support. At the age of 78 years, she eventually became bedridden in a totally locked-in state. Brain CT scan performed at the age of 81 years revealed frontotemporal atrophy (Figure 1). At the age of 85 years, the patient died of septic acute cholecystitis, about 9 years after onset of the disease. There were no parkinsonian features during the disease course. There had been no family history of ALS (MND), dementia or other neurological disease.

A general autopsy was performed about 4 h after death, at which time the brain weighed 910 g (brainstem and cerebellum, 140 g).

Neuropathological examination

The brain and spinal cord were fixed with 20% buffered formalin, and multiple tissue blocks were embedded in paraffin. Histological examinations were performed on 4-μm-thick sections using several stains: hematoxylin-eosin, Klüver-Barrera and Gallyas-Braak. In addition, selected sections were immunostained after optimal pretreatment with mouse monoclonal antibodies against hyperphosphorylated tau (AT8; Innogenetics, Ghent, Belgium; 1:200), β-amyloid (Dako; Glostrup, Denmark; 1:100; formic acid for 5 min), p62 (BD Biosciences, San Jose, CA, USA; 1:1000; microwave for 20 min), phosphorylated TDP-43 (pS409/410; Cosmo Bio, Tokyo, Japan; 1:5000; autoclave at 120 °C in 0.05 M citrate buffer for 10 min), FUS (Sigma-Aldrich, St. Louis, MO, USA; 1:50), and 3R and 4R tau (RD3 and RD4 (11); Upstate, Charlottesville, VA, USA; 1:3000 and 1:100, respectively; serial pretreatment with formic acid for 5 min and 20 min, and microwave for 20 s and 20 s, respectively), and rabbit polyclonal antibody against ubiquitin (Dako, Glostrup, Denmark; 1:800), 4R tau (anti-4R (10, 20); Cosmo

Bio, Tokyo, Japan; 1:500; serial pretreatment with formic acid for 5 min and microwave for 20 s), and phospho-PHF-tau pSer212/Thr214 (AT100; Thermo Scientific, Cergy Pontoise, France; 1: 200). Bound antibodies were visualized by the peroxidase-polymer-based method using a Histofine Simple Stain MAX-PO kit (Nichirei, Tokyo, Japan) with diaminobenzidine (DAB) as the chromogen. Immunostained sections were lightly counterstained with hematoxylin.

A double-labeling immunofluorescence study was performed on sections obtained from the precentral (motor) cortex using rabbit polyclonal anti-phosphorylated TDP-43 (pS409/410; Cosmo Bio; 1:2000) and mouse monoclonal anti-hyperphosphorylated tau (AT8; 1:2000), and with rabbit polyclonal anti-glial fibrillary acidic protein (GFAP) (Dako; 1:800) and mouse monoclonal anti-phosphorylated TDP-43 (pS409/410; Cosmo Bio; 1:2000). The second antibodies used were Alexa Fluor 488 goat anti-mouse IgG (Molecular Probes; 1:1,000) and Alexa Fluor 555 goat anti-rabbit IgG (Molecular Probes; 1:1,000), and Alexa Fluor 488 goat anti-rabbit IgG (1:1,000) and Alexa Fluor 555 goat anti-mouse IgG (1:1,000), respectively. The sections were treated with an Autofluorescence Eliminator Reagent (Millipore, Billerica, MA, USA), mounted under glass coverslips using VectaShield mounting medium with 4,6-diamidino-2-phenylindole (DAPI) nuclear stain (Vector Laboratories, Burlingame, CA, USA), and analyzed using a Carl Zeiss confocal laser scanning microscope (LSM510-V4.0).

A double-immunolabeling electron microscopy study was also carried out. Small tissue blocks of motor cortex fixed in 20% buffered formalin were embedded in LR White resin (London Resin, Reading, UK). Ultrathin sections were then cut, placed on Formvar-coated nickel grids, incubated in a mixture of GFAP (1:200) and AT8 (1:10),